Nature of small-polaron hopping conduction and the effect of Cr doping on the transport properties of rare-earth manganite La0.5Pb0.5Mn1−xCrxO3

Aritra Banerjee, S. Pal, and B. K. Chaudhuri

Citation: J. Chem. Phys. **115**, 1550 (2001); doi: 10.1063/1.1378018
View online: http://dx.doi.org/10.1063/1.1378018
View Table of Contents: http://jcp.aip.org/resource/1/JCPSA6/v115/i3
Published by the AIP Publishing LLC.

Nature of small-polaron hopping conduction and the effect of Cr doping on the transport properties of rare-earth manganite $La_{0.5}Pb_{0.5}Mn_{1-x}Cr_xO_3$

Aritra Banerjee, S. Pal, and B. K. Chaudhuri[a)]
Department of Solid State Physics, Indian Association for the Cultivation of Science, Jadavpur, Calcutta-700 032, India

(Received 8 January 2001; accepted 18 April 2001)

The conductivity and magnetoresistance of $La_{0.5}Pb_{0.5}Mn_{1-x}Cr_xO_3$ ($0.0 \leqslant x \leqslant 0.45$) measured at 0.0 and 1.5 T magnetic field have been reported. All the oxide samples except $x=0.45$, showed metal insulator transition (MIT) between 158–276 K, depending on x. In contrast to the behavior of a similar sample $La_{0.7}Ca_{0.3}Mn_{1-x}Cr_xO_3$ showing no (MIT) for $x \geqslant 0.3$, the Pb doped samples showed MIT even with $x=0.35$. The MIT peak temperature (T_p) shifts towards lower temperature with increasing x while magnetic field shifts T_p to the high temperature regime. The metallic (ferromagnetic) part of the temperature dependent resistivity (ρ) curve (below T_p) is well fitted with $\rho(T)=\rho_0+\rho_{2.5}T^{2.5}$ indicating the importance of electron–magnon interaction (second term). We have successfully fitted the high temperature ($T > \theta_D/2$, θ_D is Debye temperature) conductivity data, both in presence and in absence of magnetic field, with small polaron hopping conduction mechanism. Adiabatic small polaron hopping conduction mechanism is followed by the samples showing MIT while nonadiabatic hopping conduction mechanism is obeyed by the samples showing no MIT. The lower temperature (between T_p and $\theta_D/2$) conductivity data of all the samples can be well fitted to the variable range hopping (VRH) model similar to the case of many semiconducting transition metal oxides. Temperature dependent Seebeck coefficient data also support the small polaron hopping conduction mechanism above T_p. © *2001 American Institute of Physics.*
[DOI: 10.1063/1.1378018]

I. INTRODUCTION

The colossal magnetoresistance (CMR) behavior and other properties of some oxide materials have drawn extensive scientific and technological interest during the last decade. The well-known CMR materials are the mixed valence manganites with ABO_3 type perovskite structure, for example, $Ln_{1-y}AE_yMnO_3$ (where Ln is trivalent rare-earth element like La, Pr, etc., and AE is the bivalent alkaline earth metal, i.e., Sr, Pb, Ca, Ba, etc.).[1,2] The parent compound, $LaMnO_3$, is a paramagnetic insulator (PMI) showing a phase transition to an antiferromagnetic (AFM) phase at about 140 K. With the *A* site (here La) doping by the above-mentioned alkaline earth metal, the hole doped ($0.1 \leqslant y \leqslant 0.5$) oxide pervoskites show the ferromagnetic metallic state below the Curie temperature T_C. The transition temperature T_p, separating the insulating and metallic phase lies in the vicinity of Curie temperature T_C[1] around which resistivity decreases by several orders of magnitude under the application of magnetic field resulting the CMR effect. However, in spite of enthusiastic effort dedicated to this topic, detailed microscopic mechanism responsible for magnetic and transport properties of this oxides is not yet well understood. Though several attempts have been made to explain the magnetic and other properties considering double exchange (DE) interaction,[3] which renders Mn^{3+}–O^{2-}–Mn^{4+} bonds metallic, it has recently been emphasized that this DE mechanism alone cannot uniquely explain the available experimental data.[4] In many such samples, DE interaction between Mn^{3+} and Mn^{4+} gives rise to the simultaneous presence of ferromagnetism and metallic (FMM) behavior. In addition to the DE, a strong electron–phonon interaction giving rise to Jahn–Teller (JT) splitting of the outer *d* level plays an important role in the transport mechanism, especially at temperatures near and above T_p. One way to monitor the DE interaction is by the substitution of divalent ions at the Ln site, leading to the variation of the ratio $C=Mn^{4+}/Mn^{3+}$ which might lead to the lattice (JT) effect due to the change of *A* site ion size. Another way is by doping of transition metal–ion at the Mn site, the center for the DE mechanism, which directly influences the DE interaction and hence the transport and magnetic properties.

Recently the La–Pb–Mn–O-type system has been elaborately[1] studied because of its high magnetic ordering temperature (around room temperature). Like Mn, chromium (Cr) also exists in two valence states like Cr^{2+} and Cr^{3+}. Since the electronic configurations of Cr^{3+} and Mn^{4+} are identical, there is a possibility of substitution of Mn by Cr. In the present paper we have studied the effect of the partial substitution of Mn by Cr on the transport properties of the La–Pb–Mn–O system. Recently Barnabe *et al.*[5] showed that among various doping elements, Cr was the most efficient one to induce metal to insulator transition (MIT) in $La_{0.5}Ca_{0.5}Mn_{1-x}A_xO_3$. For the Cr doped system, the average *A* site cationic radius ($\langle r_A \rangle$) is smaller ($\sim$1.14 Å) than that of the corresponding undoped system ($\sim$1.19 Å). It is well es-

a)Author to whom correspondence should be addressed; electronic mail: sspbkc@mahendra.iacs.res.in

tablished that antiferromagnetic (AFM) ordering becomes stronger as $\langle r_A \rangle$ decreases, so that doping level at the B site (here Mn), depending on x, must be increased to counter balance the effect. Moreover as $\langle r_A \rangle$ decreases, one can see that the range of x values corresponding to FMM–PMI transition shrinks. Cabeza and co-researchers[6] recently studied a Cr doped system, viz. $La_{0.7}Ca_{0.3}Mn_{1-x}Cr_xO_3$. These authors, however, reported no metal-insulator transition (MIT) for $x \geqslant 0.3$ and they also reported very small effect of Cr on the transport property (dc conductivity). But, as the atomic radius of Pb is bigger than that of Ca, we believe that for the Cr doped La–Pb–Mn–O system, one should obtain MIT even with $x > 0.3$. This is found to be true as shown in the present paper. We observed MIT even with $x \geqslant 0.3$ (up to $x = 0.35$) in the $La_{0.5}Pb_{0.5}Mn_{1-x}Cr_xO_3$ system. We have also attempted to explain the nature of hopping conduction (adiabatic or nonadiabatic) in this and similar other systems above the corresponding MIT temperatures.

We should, however, mention that the results of transport properties reported in the present paper were on sintered bulk samples. Intergranular effects often potentially affect such measurements. But we will argue that the main findings are consequence of the effect of chromium doping on the bulk materials, and are not due to the grain boundary effects. In the following section we have succesively described, in brief, the experimental procedure and the method of characterization of the sample. Section III deals with the results and discussion. The paper ends with the conclusion.

II. EXPERIMENT

Bulk samples of $La_{0.5}Pb_{0.5}Mn_{1-x}Cr_xO_3$ ($0.075 \leqslant x \leqslant 0.45$) were prepared by standard solid state reaction method with stoichiometric amount $La_2(CO_3)_3$, PbO, $Mn(C_2H_3O_2)$ and Cr_2O_3, each of purity 99.99% as the starting materials. The mixtures of these materials were preheated in air at 500 °C for 5 h. After grinding they were sintered at 900 °C for 70 h with intermediate grounding (for 7 times). To see the effect of annealing, one sample with $x = 0.35$ was sintered at 900 °C for 48 h, which was also found to show MIT. The powders of different samples thus obtained were well ground again and then pelletized and annealed at 900 °C for 24 h. Finally the samples are furnace cooled to room temperature. The samples were characterized by x-ray diffraction with CuK_α ($\lambda = 1.541$ Å) radiation. Temperature dependent resistivity (ρ) was measured with four probe technique in the range of 425–80 K in zero and 1.5 T magnetic field similar to our earlier work.[7] All the experimental conductivity data were collected in the heating direction.

III. RESULTS AND DISCUSSION

X-ray diffraction data (Fig. 1) confirm all the samples as single phase materials. Thermal variation of electrical resistivity of the Cr doped $La_{0.5}Pb_{0.5}Mn_{1-x}Cr_xO_3$ with different concentrations $x = 0.075$, 0.15, 0.3, 0.35, and 0.45 are shown in Figs. 2(a) and 2(b). For all the samples (except the sample with $x = 0.45$ showing no MIT), resistivity (ρ) first increases with decrease in temperature, and then exhibits peak around

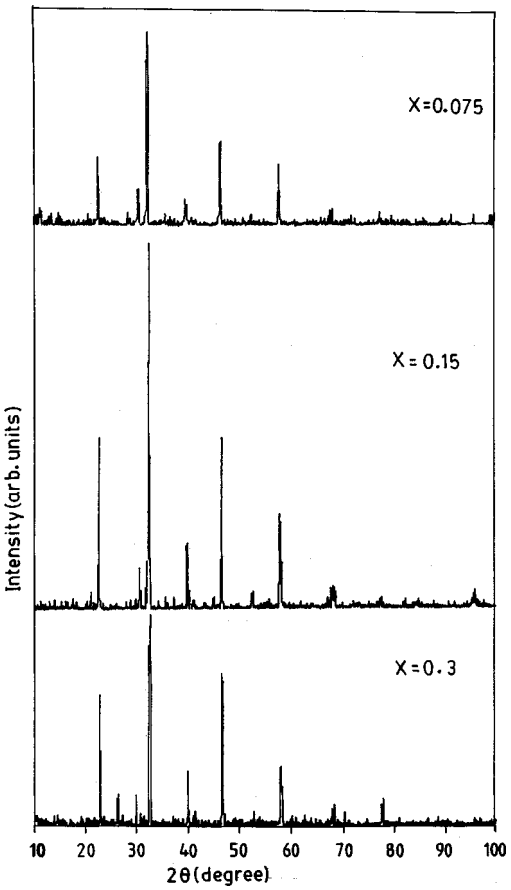

FIG. 1. X-ray diffraction patterns of three typical Cr doped $La_{0.5}Pb_{0.5}Mn_{1-x}Cr_xO_3$ samples with $x = 0.075$, 0.15, and 0.3 showing metal-insulator transitions.

the metal-insulator transition (MIT) temperature denoted by T_p. For $T > T_p$, resistivity decreases with increase of temperature. Concentrating on the behavior of temperature dependent resistivity curve, it is noted that $d\rho/dT < 0$ for $T > T_p$, which is a characteristic of semiconducting behavior. But for $T < T_p$, the sample showed metallic character with $d\rho/dT > 0$. As Cr concentration increases, resistivity also increases and T_p decreases as shown in Table I for all the samples with $x = 0-0.35$. For higher values of $x(\geqslant 0.35)$, the samples showed semiconducting behavior and no metal-insulator transition was observed as shown for a typical sample with $x = 0.45$ [Fig. 2(b)]. Figure 3 shows thermal variation of resistivity of each of the samples (showing MIT) at zero and 1.5 T magnetic field. For each sample, the value of resistivity, in presence of magnetic field, decreases and the peak temperature T_p shifts towards the high temperature region. The resistivity curves of all the samples in presence and in absence of the magnetic field, showed an uprise (Fig. 3) beyond a certain temperature (say T^*, which is around 75 K for the present samples). Similar behavior was also observed earlier in hole doped $LaMnO_3$.[8,9] The Cr free $La_{0.5}Pb_{0.5}MnO_5$ system also exhibited similar uprise of resistivity but at much lower temperature (~25 K not shown in this paper). This resistivity minimum is considered to be due to the development of interlayer antiferromagnetic coupling leading to weak localization. It appears that this material is

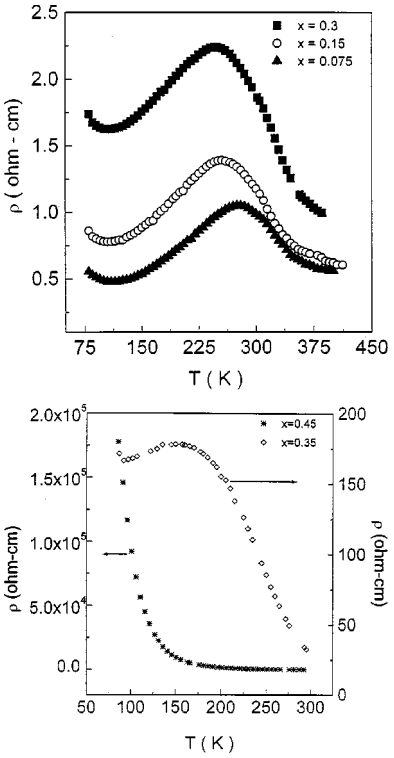

FIG. 2. Thermal variation of resistivity (ρ) of $La_{0.5}Pb_{0.5}Mn_{1-x}Cr_xO_3$ with (a) $x=0.075$(▲); 0.15 (○); and 0.3 (■) (b) $x=0.35$(*) and 0.45 (◇).

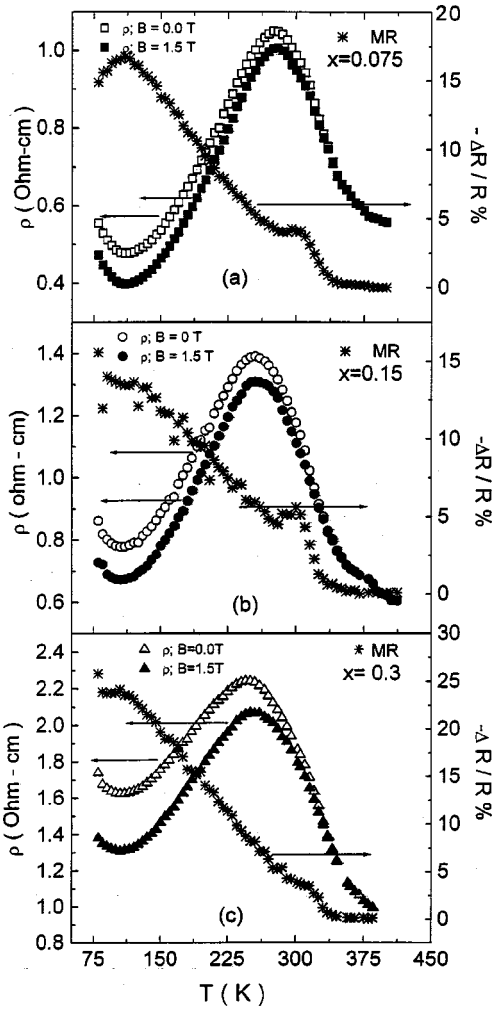

FIG. 3. Thermal variation of resistivity (ρ) and magnetoresistance for $La_{0.5}Pb_{0.5}Mn_{1-x}Cr_xO_3$ with $x=$(a)0.075, (b) 0.15, and (c) 0.3 at magnetic field $B=0.0$ and $B=1.5$ T.

not a highly homogeneous ferromagnet but can have ferromagnetically aligned clusters in a paramagnetic or antiferromagnetic matrix and depending on the size of the clusters, T^* shifts to the lower or higher temperature regime. Clusters themselves may be conducting but their concentration is small enough to make the whole sample ferromagnetic and electrically conducting. The cluster to cluster tunneling of the localized electrons/holes occurs again by hopping process giving rise to semiconducting behavior.

In order to explain the transport properties of the $LaMnO_3$-type system, one must assume that electronic structure of the doping element must play a crucial role. The present result in the DE framework suggests that Cr^{3+} must be partly ferromagnetically coupled to the Mn^{3+} and Mn^{4+} species. The doped Cr is a neighbor of Mn in the periodic table and it is generally believed that in the manganese oxides with perovskite structure, these elements exist in the form of Cr^{3+}, Mn^{3+}, and Mn^{4+}.[10] Their electronic configurations are Cr^{3+}:$t_{2g}^3(S=3/2)$, Mn^{3+}:$t_{2g}^3e_g^1(S=2)$ and Mn^{4+}:$t_{2g}^3(S=3/2)$, among which only the e_g^1 electron of Mn^{3+} is electronically active. The ionic radii of Cr^{3+}, Mn^{3+}, and Mn^{4+} are 0.615, 0.645, 0.530 Å, respectively.[11] Due to nearly the same ionic radius, the doped Cr ions replace Mn^{3+} ions in the form of Cr^{3+}. Cr^{3+} has the same electronic configuration (t_{2g}^3) as Mn^{4+} and hence there should be FM double exchange (FMDE) interaction between Mn^{3+} and Cr^{3+} just as that between Mn^{3+} and Mn^{4+}. It is evident that

TABLE I. Some important estimated parameters of the $La_{0.5}Pb_{0.5}Mn_{1-x}Cr_xO_3$ for different values of x. ρ_{rt}(ohm cm) = resistivity and S = grain size at 300 K. To see the effect of annealing time, the sample with $x=0.35$ was prepared with lower annealing time (48 h) instead of 70 h used for other samples (with $x=0.075-0.45$).

x	S (μm)	r_p (Å)	R (Å)	N (cm^{-3})	θ_D (K)	ν_{ph} (Hz)	ρ_{rt}(ohm cm)	T_p (K)
0.075	6.28	2.089	5.183	7.182×10^{21}	625.00	1.293×10^{13}	0.975	276.11
0.150	5.69	2.023	5.019	7.909×10^{21}	612.24	1.267×10^{13}	1.158	256.11
0.300	2.74	1.982	4.918	8.4×10^{21}	606.06	1.254×10^{13}	1.880	245.00
0.350	⋯	2.041	5.060	7.7×10^{21}	467.40	9.67×10^{13}	32.270	158.90
0.450	⋯	1.954	4.849	8.769×10^{21}	411.80	8.519×10^{13}	977.900	⋯

the presence of Cr^{3+} in the Mn^{3+}–O–Mn^{4+} network disturbs the lattice (increase of electron–phonon interaction) favoring the formation of polarons and hopping occurs between the different valence states of Mn in the insulating (semiconducting) phase. Several recent studies have suggested that the nature of the charge carriers responsible for transport in such systems above T_p are localized.[12–18] The charge localization leads to a temperature dependence of ρ which can be described by two distinct aspects viz. charge localization due to lattice distortion (small polaron formation) and the variable range hopping in a Coulomb gap. On the other hand, in the low temperature phase, where ordering of the carriers (charge ordering in some cases) takes place in the Mn network, favoring electron hopping from Mn^{3+} to Mn^{4+} sites leading to the FMM state due to double exchange. This proposal also supports some experimental results.[19] Hence with Cr doping in the La–Pb–Mn–O system, Mn^{3+}/Mn^{4+} ratio decreases (as Cr^{3+} acts as Mn^{4+}). But it is also known that Cr^{3+}–Mn^{3+} FMDE interaction is smaller than that of Mn^{3+}–Mn^{4+}.[20] Hence with Cr doping, the effective FMDE interaction becomes weaker, resulting in the gradual decrease of T_p with increasing Cr concentration. Also due to weaker DE interaction, the only electronically active electron, e_g^1 electron of Mn^{3+} ion, become localized, causing the gradual increase in resistivity[21] of $La_{0.5}Pb_{0.5}Mn_{1-x}Cr_xO_3$ with increasing concentration x (Fig. 2).

From Fig. 3 one finds that the resistivity decreases but T_p shifts to higher temperature with the application of magnetic field. The Cr substitution may also favor the charge carrier delocalization induced by the magnetic field, which suppresses the resistivity. The application of the magnetic field (B), also causes the local ordering of magnetic spin and due to this ordering, the ferromagnetic metallic (FMM) state suppresses the paramagnetic insulating (PMI) state and hence the peak temperature (T_p) shifts to the high temperature regime with application of magnetic field. Cao *et al.*[22] also explained this phenomenon in terms of ferromagnetic clusters or domain.

As observed from Fig. 2(a), conductivity data showed metallic behavior below the MIT temperature T_p. From the survey of recent literature,[13,21,23–25] one finds that the temperature dependent resistivity data of the rare-earth manganite system, below T_p, is not well understood. In order to analyze the resistivity data below T_p, we first take account of the metallic part between T_p and T^*. The experimental data within this temperature range (below T_p) has been attempted to fit with different expressions for resistivity [Eqs. (1)–(3) below] derived by different authors.[13,21,23–25] Such fitting would help to find which model is best suited for the present system as well as the nature of interaction. The proposed resistivity–temperature relations are (for $T<T_p$)

$$\rho=\rho_0+\rho_2T^2, \tag{1}$$

$$\rho=\rho_0+\rho_2T^2+\rho_{4.5}T^{4.5}, \tag{2}$$

$$\rho=\rho_0+\rho_{2.5}T^{2.5}, \tag{3}$$

where the temperature independent part ρ_0 is the resistivity due to domain, grain boundary and other temperature independent scattering mechanism.[13,23] ρ_2T^2 term corresponds to the electron–electron scattering process[13,24] and it is dominant in the range up to 100 K.[13] Though Snyders *et al.*[13] described the $\rho_{4.5}T^{4.5}$ term as a contribution from the electron–magnon scattering process, actually it might be due to the spin wave scattering in the ferromagnetic phase[24] and the electron–magnon scaterring process contributes in the $\rho_{2.5}T^{2.5}$ term as suggested by another research group.[21,23] This electron–magnon scattering term is important in the low temperature region [below T_p (Refs. 13, 21, and 23)]. We have first tried to fit the metallic part of the resistivity curve (shown between T_p and T^*) with all these three empirical equations containing, as discussed above, the electron–electron, electron–phonon, and electron–magnon scattering terms which are expected to be significant also for the present system.[25] We find that in the metallic regime, conductivity data for all the samples showing MIT best fit the equation $\rho=\rho_0+\rho_{2.5}T^{2.5}$, both in presence and in absence of the magnetic field. Figure 4 shows that the low temperature $\rho\sim T^{2.5}$ curve is almost linear which suggests that the transport mechanism in this regime can be attributed to the electron–magnon scattering, which further demonstrates[21] that the metallic regime is actually in the ferromagnetic (FM) phase. Here we should mention that the electron–phonon interaction seemed to be not very important in the low temperature region. Typically, in metal, the strength of the electron–phonon interaction is such that the $\Delta\rho(\approx 300\,\mathrm{K})[=\rho_{300\,K}-\rho_{4.2\,K}]\leqslant 100\,\mu\Omega\,\mathrm{cm}$. In metallic oxides $\Delta\rho(\approx 300\,\mathrm{K})$ is typically $\leqslant 1$–$3\,\mathrm{m}\Omega\,\mathrm{cm}$. In the manganates, although $d\rho/dT>0$ in the region $T<T_p$, as a conventional metal, the temperature dependence of ρ measured as $\Delta\rho(T_c)[=\rho_{300\,K}-\rho_{4.2\,K}]$ is much larger. For example, in $La_{1-x}Ca_xMnO_3$ and $LaMnO_3$ samples, the observed $\Delta\rho \approx 3$–$4\,\Omega\,\mathrm{cm}$. In the present Cr doped La–Pb–Mn–O system, this value is of similar order in magnitude. Such large values of $\Delta\rho$ has to arise from unusually large electron–phonon coupling constant. One can, therefore, rule out the importance of electron–phonon interaction for the explanation of temperature dependence of ρ in the low temperature region. The best fit parameters obtained from fitting of the low temperature metallic part of the conductivity data with Eq. (3) (both in zero and 1.5 T magnetic field) are shown in Table II. As expected, the temperature independent term for all the polycrystalline samples is somewhat larger than those obtained for films or single crystals.[25] One finds from Table II that ρ_0 decreases significantly with magnetic field, but the influence of field on the $\rho_{2.5}$ term is very small. It is likely that the main mechanism responsible for magnetoresistance is the influence of magnetic field on the magnetic domains. As magnetic field increases, the size of the domain boundary decreases and ρ_0 becomes smaller.[25] The slight decrease of $\rho_{2.5}$ in a magnetic field may be due to the suppression of spin fluctuation in the applied magnetic field (proportional to $H^{-1/3}$).[13]

It is further observed that in the high temperature insulating (semiconducting) regime (above the MIT temperature T_p), the conductivity data can be well fitted with the small polaron hopping model due to Mott[26] which was also followed by similar other samples.[1,6,13,21,22] It is also found that high temperature (above T_p) transport property in the rare-

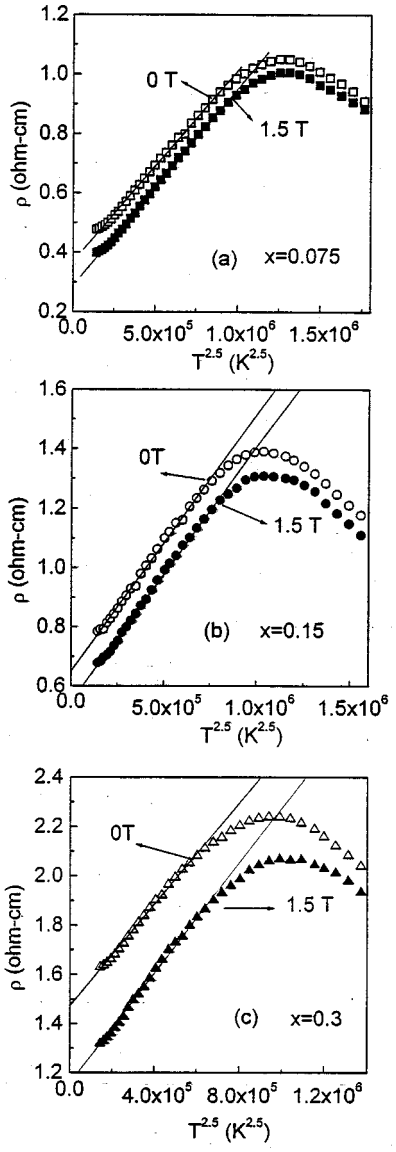

FIG. 4. Resistivity (ρ) vs $T^{2.5}$ curve for $La_{0.5}Pb_{0.5}Mn_{1-x}Cr_xO_3$ with x = (a)0.075, (b) 0.15, and (c) 0.3 below the metal-insulator transition (MIT) temperature T_p both in the presence and in the absence of magnetic field. The solid lines give the best fit to Eq. (3) at lower temperatures ($T<T_p$).

earth manganite system is dominated by the thermally activated hopping of a small polaron.[13–15] According to the small polaron hopping model, the expression for conductivity is given by the relation

$$\rho/T=\rho_\alpha \exp(E_p/k_BT), \tag{4}$$

TABLE II. The values of the parameters ρ_0 and $\rho_{2.5}$ obtained from fitting the low temperature ($T<T_p$) conductivity data with Eq. (1) both in presence and in absence of magnetic field.

	ρ_0 (ohm cm)		$\rho_{2.5}$ (ohm cm $K^{-2.5}$)	
x	0 T	1.5 T	0 T	1.5 T
0.075	0.3697	0.2883	6.42×10^{-7}	6.63×10^{-7}
0.15	0.6506	0.5473	8.64×10^{-7}	8.58×10^{-7}
0.30	1.1573	1.4743	1.12×10^{-6}	1.03×10^{-6}
0.35	159.47	125.8825	8.00×10^{-5}	1.00×10^{-4}

where, $\rho_\alpha=[k_B/\nu_{ph}Ne^2R^2C(1-C)]\exp(2\alpha R)$, k_B is the Boltzmann constant and T is the absolute temperature. N is the number of ion sites per unit volume, R is the average intersite spacing obtained from the relation $R=(1/N)^{1/3}$, C is the fraction of sites occupied by a polaron, α is the electron wave function decay constant obtained from fitting the experimental conductivity data, ν_{ph} is the optical phonon frequency. E_p is the activation energy given by the relation[27]

$$E_p=W_H+W_D/2 \quad (\text{for } T>\theta_D/2)$$

$$=W_D \quad (\text{for } T<\theta_D/4)$$

where W_H is the polaron hopping energy, W_D is the disorder energy, and θ_D is the Debye temperature. The estimated values of R are given in Table I. W_H (Table III) is obtained from the relation[8] $W_H=E_p-E_s$, where E_s is the activation energy obtained from fitting of the thermoelectric power vs temperature curves (not discussed in this paper; the estimated values of E_s are given in Table III). We replotted the resistivity curves as $\ln(\rho/T)-1/T$ (Fig. 5) and from the slope of the straight line curve above $\theta_D/2$, we have calculated the activation energy E_p (Table III). Figure 5 predicts the temperature dependence of activation energy above the respective values of $\theta_D/2$ (high temperature linear part). The values of $\theta_D/2$ are estimated from the temperature where deviation from linearity occurs in the high temperature region as shown in Fig. 5.

It is observed from Table III that with increasing x, i.e., Cr concentration, the activation energy (E_p) gradually increases. It is obvious that with the increase of Cr concentration, the number of e_g electrons of Mn^{3+} become more localized (discussed above), which increases the activation energy.[21] We have also fitted, for the first time, the high temperature resistivity data obtained in the presence of magnetic field with Eq. (4) and from the slope of the straight line curve in Fig. 5, we have calculated the corresponding field dependent activation energy (shown in Table III). It is observed that even in magnetic field, E_p increases with x, similar to the case of zero magnetic field, but for each concentration (x), E_p decreases in presence of the field. This can be explained on the basis of delocalization of e_g electron in magnetic field, discussed above. It is further noticed that the resistivity (above $\theta_D/2$) data can be well fitted with Eq. (4) for $\exp(2\alpha R)=1$ (indicating $\alpha=0$ as $R\neq0$). When the overlap integral $J_0\exp(2\alpha R)$ between the sites approaches J_0, the hopping is adiabatic.[26] This suggests adiabatic conduction mechanism is valid for all samples showing MIT for $T>\theta_D/2$. It is, however, always difficult to uniquely identify the nature of the hopping conduction mechanism if only temperature dependence of conductivity is used, because the conductivity subject to the adiabatic small polaron conduction also satisfies the temperature dependence of nonadiabatic conduction. It has been shown below, using other theoretical consideration, that depending on concentration, different conduction mechanisms (adiabatic and nonadiabatic) are followed by these manganite samples in the high temperature ($T>T_p$) regime.

It is well known[26] and also mentioned above that conductivity data of semiconducting oxide system in the low

TABLE III. The values of activation energies estimated from conductivity (E_p) and thermoelectric power (E_s) of $La_{0.5}Pb_{0.5}Mn_{1-x}Cr_xO_3$ in presence and in absence of magnetic field. The estimated values of dielectric constant (ε) and electron–phonon interaction constant (γ) are also shown for different samples.

	E_p (meV)		E_s (meV)		$W_H = E_p - E_s$ (meV)		ε		
x	0 T	1.5 T	0 T	1.5 T	0 T	1.5 T	0 T	1.5 T	$\gamma = 2W_H/h\nu_{ph}$
0.075	111.56	102.98	11.49	10.85	100.07	92.13	10.28	11.17	3.72
0.15	117.47	108.73	14.7	13.49	102.78	95.25	10.34	11.15	3.9
0.3	123.00	115.64	8.31	8.05	114.69	107.59	9.46	10.08	4.39
0.35	147.85	141.24	10.85	10.05	137.0	131.19	7.682	8.022	6.797
0.45	172	169.97	13.82	13.05	158.85	156.91	6.954	7.01	8.908

temperature regime (below $\theta_D/2$) follow Mott's variable range hopping (VRH) model of the charge carriers. Recently Pi *et al.*,[21] Jaime *et al.*,[18] and Viret *et al.*[28] also applied this model in similar systems like $La_{0.825}Sr_{0.175}Mn_{1-x}Cu_xO_3$, La–Ca–Mn–O, etc., for all temperatures above the MIT temperature T_p. But in reality, the VRH model [Eq. (5) below] was derived[26] for explaining the conductivity data below $\theta_D/2$. So we attempted to apply the VRH model, shown below [Eq. (5)], to fit the experimental conductivity data of the present manganites in the low temperature range (between $\theta_D/2$ and T_p) as shown in Fig. 6. It is seen from the VRH model [Eq. (5) below] that this model fits the conductivity data in this range of temperature quite well. Similarly, we have also tried, for the first time, to fit the conductivity data in the same temperature region ($T_p < T < \theta_D/2$) obtained in presence of a magnetic field of 1.5 T [Figs. 6(b), 6(d), 6(f)]. Here also we noticed good fitting of the data with Eq. (5) is valid for the semiconducting phase ($T > T_p$). According to the VRH model, the expression for dc conductivity in the 3D case can be written in the form[29]

$$\sigma = \sigma_0 \exp(-T_0/T)^{1/4}, \tag{5}$$

where T_0 is a constant $= 16\alpha^3/K_B N(E_F)$, $N(E_F)$ the density of states at the Fermi level is calculated from the slope of $\log \sigma$ vs $T^{1/4}$ graph (Fig. 6). The estimated value of $N(E_F)$ both in the presence and in the absence of the magnetic field are shown in Table IV. Recently Viret *et al.*[28] estimated $\alpha = 2.22\,\mathrm{nm}^{-1}$ for La–Sr–Mn–O samples showing MIT. To estimate the values of $N(E_F)$ (as given in Table IV), we also use $\alpha = 2.22\,\mathrm{nm}^{-1}$ for best fitting with Eq. (5). It is noticed that the $N(E_F)$ values increase in the presence of magnetic field for all Cr concentration (Table IV) and $N(E_F)$ is also two to three orders of magnitude higher in these manganites than those of usual oxide semiconductors.[26] Such a higher value of $N(E_F)$ also estimated by other researchers,[28,30] is due to the higher conductivity of these oxides than those of the usual transition-metal–oxide semiconductors[29,31] and this large value of $N(E_F)$ is also an indication of adiabatic hopping behavior of the carriers in these manganites as pointed out by Jung.[30] Interestingly, for the semiconducting sample ($La_{0.5}Pb_{0.5}Mn_{1-x}Cr_xO_3$ with $x = 0.45$) without exhibiting MIT, $N(E_F)$ is smaller $\sim 10^{19}$ (Table IV) and comparable to many oxide semiconductors. Thus we noticed that the semiconductor to metallic transition which is associated with the change of concentration (x) is also related to the change of the conduction mechanism. We also estimated the values of the prefactor σ_0 in Eq. (5) which varied from 17 to 20 $\mathrm{m\Omega\,cm}$, depending on the Cr concentrations. This value of the prefactor obtained from Mott's equation[32] is of the order of $\rho_{\mathrm{Mott}} = 10\,\mathrm{m\Omega\,cm}$, which indicates the validity of VRH. Jung,[30] however, estimated $\rho_{\mathrm{Mott}} = 1.087 \times 10^{-11}\,\mathrm{m\Omega\,cm}$ which is unphysical. This discrepancy in comparison to our calculations arise due to to fact that Jung fitted the dc conductivity data of La–Ca–Mn–O system for the entire range

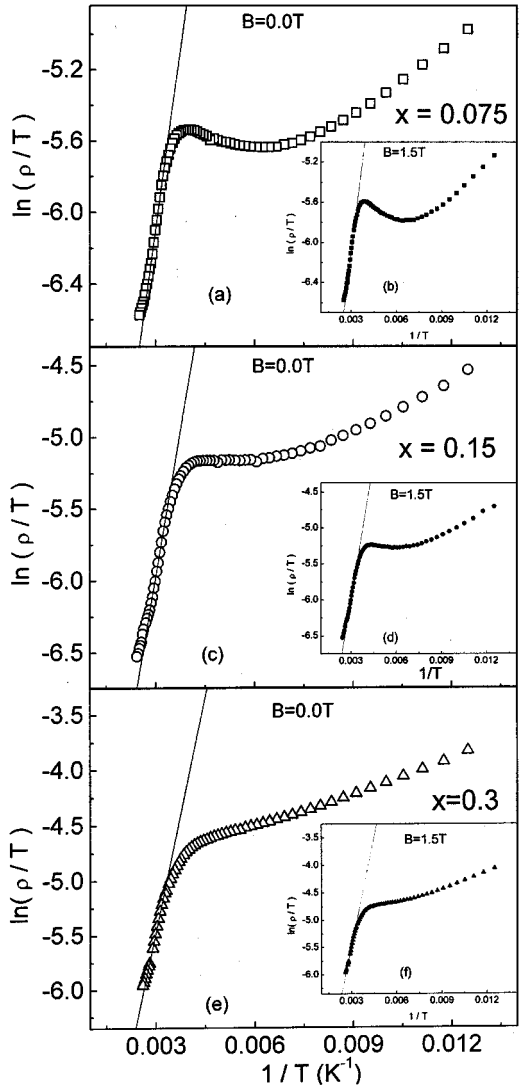

FIG. 5. Variation of $\ln(\rho/T)$ as a function of inverse temperature $1/T$ for $La_{0.5}Pb_{0.5}Mn_{1-x}Cr_xO_3$ with $x = 0.075$ (a) and (b); $x = 0.15$ (c) and (d); $x = 0.3$ (e) and (f) above the metal-insulator transition (MIT) temperatures. The inset curves (b), (d), (f) represent the data taken in presence of magnetic field $B = 1.5$ T. Solid lines are the best fit to the Mott's SPH model [Eq. (4)].

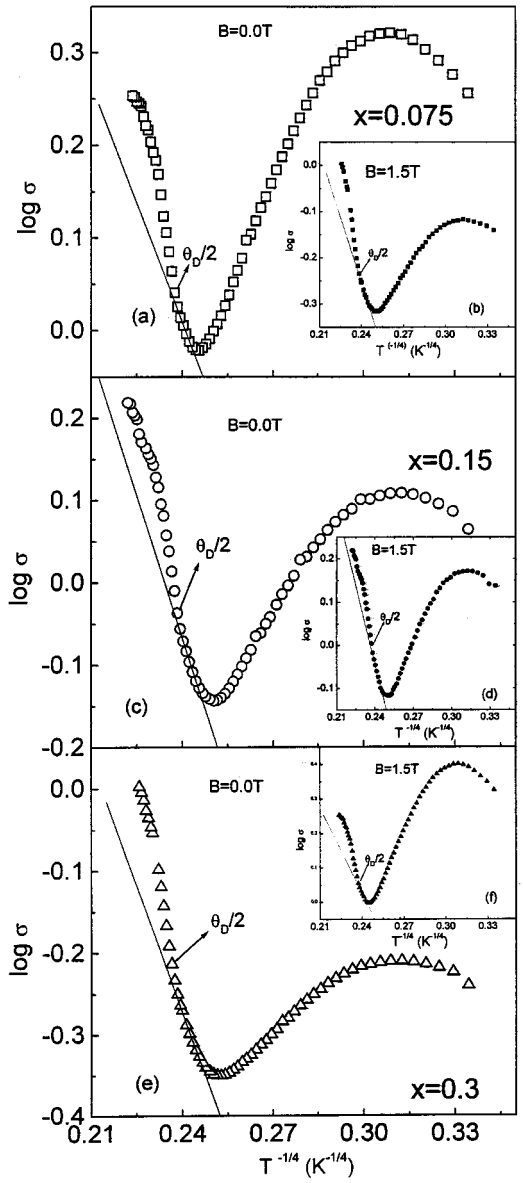

FIG. 6. Plot of $\log \sigma$ vs $T^{1/4}$ for $La_{0.5}Pb_{0.5}Mn_{1-x}Cr_xO_3$ with $x=0.075$ (a) and (b); $x=0.15$ (c) and (d); $x=0.3$ (e) and (f) [insets curve (b), (d), (f) are taken in presence of magnetic field $B=1.5$ T] between T_p and $\theta_D/2$ (where θ_D is the Debye temperature). The solid line corresponds to the best fit curve with Mott's VRH model [Eq. (5)].

of temperature above T_p which is considered to be not correct. The VRH, for such system, should actually be valid between T_p and $\theta_D/2$ as discussed above. Value of $\theta_D/2$ is well above T_p.

As pointed out earlier in this paper, one can also confirm, the nature of the hopping conduction (adiabatic or nonadiabatic) from the Holstein's condition[33] discussed below. According to this condition the polaron band width J should satisfy the inequality $J>\phi$ (for adiabatic condition) and $J<\phi$ (for nonadiabatic condition) where

$$\phi=(2K_BTW_H/\pi)^{1/4}(h\nu_{\mathrm{ph}}/\pi)^{1/2}. \tag{6}$$

Using the values of W_H and ν_{ph} from Tables I and III, the estimated values of ϕ are given in Table IV. The J values are calculated independently from the model proposed by Mott

TABLE IV. Values of density of states at the Fermi level $N(E_F)$ both in presence and in absence of magnetic field (1.5 T), and other parameters J and ϕ [Eq. (6)] estimated for different concentrations (x) of the samples $La_{0.5}Pb_{0.5}Mn_{1-x}Cr_xO_3$.

	$N(E_F)$ ($eV^{-1}cm^{-3}$)		J (eV)		ϕ (eV)
x	0 T	1.5 T	0 T	1.5 T	0 T
0.075	1.63×10^{22}	1.84×10^{22}	0.212	0.198	0.0264
0.15	5.01×10^{21}	4.15×10^{21}	0.116	0.095	0.0263
0.3	7.97×10^{21}	1.10×10^{22}	0.167	0.179	0.0269
0.35	2.21×10^{19}	1.49×10^{21}	0.0989	0.113	0.0247
0.45	4.17×10^{19}	4.57×10^{19}	0.0193	0.0199	0.0214

and Davis[26] viz. $J\sim e^3[N(E_F)/\varepsilon^3]^{1/2}$. Dielectric constant of the samples ε is calculated from the relation[26] $W_H=e^2/4\varepsilon(1/r_p-1/R)$ where r_p is the polaron radius. Using the estimated values of $N(E_F)$ and ε (from Table III), the calculated values of J are given in Table IV. Comparing these values of J and ϕ, it is observed that the condition $J>\phi$ is well satisfied for all the samples (except the semiconducting sample with $x=0.45$). Thus, above T_p, adiabatic hopping conduction is valid for all these Cr doped samples showing MIT. On the other hand, for the semiconducting sample ($x=0.45$) without showing MIT, $J<\phi$ indicates the nonadiabatic hopping conduction mechanism. We showed earlier[34] that the stoichiometric $LaMnO_3$ sample without exhibiting MIT also followed nonadiabatic hopping condition in the same high temperature regime (above $\theta_D/2$). Depending on Mn concentration, the adiabatic hopping condition was also reported earlier.[3,35]

The observed change of conduction mechanism with temperature is well visualized from Fig. 7 where we have replotted the zero-field resistivity curve of a typical Cr-doped sample as a function of temperature in the range 250–400 K. This extended curve shows that there are three well-defined linear regions, *AB, BC, CD* with three different slopes. As discussed above, we have fitted only the region *BC* (above $\theta_D/2$) with SPH model (Fig. 5) and the region *AB* (between $\theta_D/2$ and T_p) with VRH model (Fig. 6). But the region *CD* remains unexplained. We suggest that some other model, probably nonadiabatic small polaron hopping model, as in

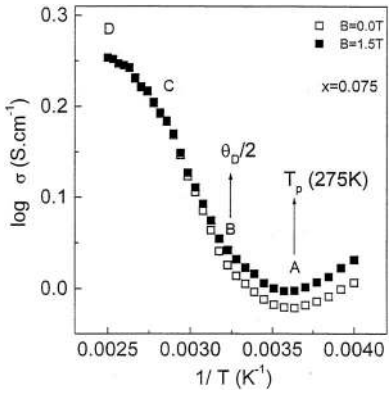

FIG. 7. Variation of $\log \sigma$ with inverse temperature for the $La_{0.5}Pb_{0.5}Mn_{0.925}Cr_{0.075}O_3$ system both in absence (□) and in presence of magnetic field $B=1.5$ T (■) showing three different linear regions, *AB*, *BC*, and *CD* above the metal-insulator transition temperature T_p.

the case of $LaMnO_3$, should also be valid in this high temperature regime (*CD*). Further work with extended temperature range is needed to confirm the transport mechanism in this regime.

Again electron–phonon ($e-$ph) coupling constants (γ) of the samples were calculated using the relation[26,27] $\gamma = 2W_H/h\nu_{\rm ph}$. From theoretical calculations Millis *et al.*[4] argued that the $e-$ph coupling constant γ is the crucial parameter controlling T_C which is in the vicinity of T_p for our samples: increasing γ decreases T_C (or T_p). It is seen from Table I that for the samples of our present investigation viz. $La_{0.5}Pb_{0.5}Mn_{1-x}Cr_x$, T_p decreases with increasing γ. This supports the theory proposed by Millis *et al.*[4]

For completeness sake, we discussed below, about magnetoresistance (MR) of the samples of our present investigation. Figure 3 indicated the thermal variation of MR [$-\Delta R/R_0 = -(R_H - R_0)/R_0 \times 100\%$, where R_H = resistance in a field of 1.5T, R_0 = resistance at zero field] of three samples showing MIT. All the samples showed small anomaly around T_p and MR grew rapidly with decreasing temperature (below T_p). With increasing Cr concentration, the maximum value of MR increases gradually. This behavior of the temperature dependent magnetoresistance curve agrees with those of other similar samples.[36,37]

Finally, in order to find the effect of grain size on resistivity and MR we calculated the grain sizes of the three typical ($0.075 < x < 0.3$) samples from the XRD data, using the relation $S = K\lambda/\beta\cos(2\theta)$,[38] where K is a constant depending on the grain shape ($=0.89$, assuming circular grain), λ = wavelength of the CuK_α radiation = 1.541 Å and β = full width at half maxima (FWHM) of XRD peak. From the estimated average grain size presented in Table I one finds that with increasing Cr concentration, grain size decreases. Moreover, it is also observed that resistivity increases but T_p decreases with decreasing grain size. The maximum value of MR also increases gradually with decreasing grain size. Similar grain size dependent MR has also been observed in other polycrystalline samples reported earlier[2,17,21,36] and was attributed to spin dependent grain boundary scattering in the low temperature region (below MIT temperature).

IV. SUMMARY AND CONCLUSION

Single phase Cr doped rare-earth manganite $La_{0.5}Pb_{0.5}Mn_{1-x}Cr_xO_3$ has been prepared to study the effect of Cr doping on the metal-insulator transition temperature and electrical resistivity both in presence and in absence of magnetic field. Interestingly, we note that unlike $La_{0.7}Ca_{0.3}Mn_xCr_{1-x}O_3$ (showing no MIT for $x \geq 0.3$), MIT is observed with higher values of x the present samples $La_{0.5}Pb_{0.5}Mn_{1-x}Cr_xO_3$ (even with $x = 0.35$). The conductivity also depends on the Cr concentration and showed little decrease with increase of Cr content in the sample which we consider to be due to the formation of impurity bonds like Cr–Mn–Mn and Cr–O–Cr. These impurity bonds also effect the magnetic interaction in this system and become effective well below the spin ordering temperature. Conductivity data above the $\theta_D/2$ (in the high temperature semiconducting regime) can be well explained by adiabatic small polaron hopping model for the samples showing MIT. Interestingly, for the semiconducting sample (with $x = 0.45$) without showing MIT, nonadiabatic hopping condition is valid for this high temperature ($T > \theta_D/2$) range. However, in the lower temperature range (between $\theta_D/2$ and T_p), conductivity data of all the samples are well fitted with the VRH model [Eq. (5)]. This behavior of temperature dependent conductivity above T_p resembles that of many oxide semiconductors.[26,31] For the samples showing MIT, the density of states at the Fermi level $N(E_F)$ is 2–3 orders of magnitude higher than those of many transition-metal–oxide semiconductors.[26] In the low temperature regime, below the metal-insulator transition ($T < T_p$), resistivity follows a relation $\rho = \rho_0 + \rho_{2.5}T^{2.5}$, suggesting the importance of electron–magnon interaction. The thermoelectric power (TEP) data (not presented in this paper) of all the samples showed anomaly around T_p and appreciable magnetic field dependence around the transition region. The TEP data also suggested (from the calculation of activation energy) small polaron hopping conduction in the high temperature regime (above $\theta_D/2$) for all the Cr doped manganites. The estimated values of localization length ($1/\alpha$), hopping radius (R), electron–phonon interaction constant, hopping energy, etc., governing the high temperature transport property are found to be reasonable for polaron hopping conduction in the Cr doped La–Pb–Mn–O-type rare-earth manganites.

ACKNOWLEDGMENT

The authors are grateful to the Department of Science and Technology, Govt. of India for financial assistance.

[1] R. Mahendiran, R. Mahesh, A. K. Roy Chaudhuri, and C. N. R. Rao, J. Phys. D **28**, 1743 (1995).
[2] R. Mahendiran, R. Mahesh, A. K. Roy Chaudhuri, and C. N. R. Rao, Solid State Commun. **99**, 149 (1996).
[3] C. Zener, Phys. Rev. **82**, 403 (1951).
[4] A. J. Millis, B. I. Shraiman, and R. Mueller, Phys. Rev. Lett. **77**, 175 (1996).
[5] A. Barnabe, A. Maignan, M. Hervieu, F. Damay, C. Martin, and B. Raveau, Appl. Phys. Lett. **71**, 3907 (1997).
[6] O. Cabeza, M. Long, C. Severae, M. A. Bari, C. M. Muirhead, M. G. Fransisconi, and G. Greaves, J. Phys.: Condens. Matter **11**, 2569 (1999).
[7] A. I. Shames, E. Rozenberg, G. Gorodetski, J. Pellegand, and B. K. Chaudhuri, Solid State Commun. **107**, 91 (1998).
[8] R. Mahendiran, S. K. Tiwary, A. K. Roy Chaudhuri, T. V. Ramakrishna, R. Mahesh, N. Rangavittal, and C. N. R. Rao, Phys. Rev. B **53**, 3348 (1996).
[9] A. Chakraborty, D. Bhattacharya, and H. S. Maiti, Phys. Rev. B **56**, 8828 (1997).
[10] J. Zhang, Q. Yan, F. Wang, P. Yuan, and P. Z. Hang, J. Phys.: Condens. Matter **12**, 1981 (2000).
[11] P. V. Vanitha, R. S. Singh, S. Natarajan, and C. N. R. Rao, J. Solid State Chem. **137**, 365 (1998).
[12] H. Y. Hwang, S. W. Cheong, P. G. Radaelli, M. Marezio, and B. Batlogg, Phys. Rev. Lett. **75**, 914 (1995).
[13] G. Jeffrey Snyder, R. Hiskes, S. Dicarolis, M. R. Beasley, and T. H. Geballe, Phys. Rev. B **53**, 14434 (1996).
[14] C. H. Booth, F. Bridge, G. J. Snyder, and T. H. Geballe, Phys. Rev. B **54**, R15606 (1996).
[15] A. J. Milles, P. B. Littelewood, and B. I. Shraiman, Phys. Rev. Lett. **74**, 5144 (1995).
[16] A. J. Milles, Phys. Rev. B **53**, 8434 (1996).
[17] A. Gupta *et al.*, Phys. Rev. B **54**, R15629 (1996).
[18] M. Jaime, M. B. Salamon, M. Rubienstein, R. E. Treece, J. S. Horwitz, and D. B. Chrisey, Phys. Rev. B **54**, 11914 (1996).
[19] P. V. Vanitha, R. S. Singh, S. Natarajan, and C. N. R. Rao, Solid State Commun. **109**, 135 (1999).

[20] A. Maignan, C. Martin, F. Damay, M. Hervieu, and B. Raveau, J. Magn. Magn. Mater. **188**, 185 (1998).
[21] L. Pi, L. Zhang, and Y. Zhang, Phys. Rev. B **61**, 8917 (2000).
[22] X. W. Cao, J. Fang, and K. B. Li, Solid State Commun. **115**, 201 (2000).
[23] J. M. De Teresa, M. R. Ibarra, J. Blasco *et al.*, Phys. Rev. B **54**, 1187 (1996).
[24] A. Urushibara, Y. Moritomo, T. Arima *et al.*, Phys. Rev. B **51**, 14103 (1995).
[25] P. Schiffer, A. P. Ramirez, W. Bao, and S. W. Cheong, Phys. Rev. Lett. **75**, 3336 (1995).
[26] N. F. Mott and E. A. Davis, in *Electronics Process in Noncrystalline Materials* (Clarendon, Oxford, 1971).
[27] G. N. Austin and N. F. Mott, Adv. Phys. **18**, 41 (1969).
[28] M. Viret, L. Ranno, and J. M. D. Coey, Phys. Rev. B **55**, 8067 (1997).
[29] N. F. Mott, J. Non-Cryst. Solids **1**, 1 (1968).
[30] W. H. Jung, J. Mater. Sci. Lett. **17**, 1317 (1998).
[31] S. R. Elliott, Adv. Phys. **36**, 135 (1987).
[32] N. F. Mott, *Metal Insulator Transitions* (Taylor and Francis, London, 1974).
[33] T. Holstein, Appl. Phys. (N.Y.) **8**, 343 (1959).
[34] S. Pal, A. Banerjee, E. Rozenberg, and B. K. Chaudhuri, J. Appl. Phys. **89**, 4955 (2001).
[35] S. Chatterjee, P. H. Chou, I. P. Houg, and H. D. Yang, Phys. Rev. B **61**, 6106 (2000).
[36] H. L. Ju and H. Sohn, Solid State Commun. **102**, 463 (1997).
[37] X. W. Xu, L. Baohe, Q. Zheng, and J. Han-min, J. Appl. Phys. **86**, 5164 (1999).
[38] A. Taylor, *X-ray Metallography* (Wiley, New York, 1961).